2020 American Control Conference
Denver, CO, USA, July 1-3, 2020

Adaptive Control of Discrete-Time Systems with Unknown, Unstable Zero Dynamics

Syed Aseem Ul Islam, Tam W. Nguyen, Ilya V. Kolmanovsky, and Dennis S. Bernstein

***Abstract*— Adaptive control of systems with poorly known or unmodeled unstable zero dynamics remains a challenging problem. This paper presents an extension of retrospective cost adaptive control (RCAC) called data-driven RCAC (DDRCAC), which does not require that the zero dynamics be known a priori. Instead, the method uses online identification to obtain an approximate model of the plant numerator dynamics for use in the target model of RCAC. DDRCAC is demonstrated numerically on systems with linear and nonlinear unstable zero dynamics that are a priori unknown.**

I. Introduction

Systems with unstable zero dynamics arise in many applications [1]. For linear systems, unstable zero dynamics manifest themselves as nonminimum-phase (NMP) zeros. For nonlinear systems, the zero dynamics are characterized by control inputs that make the output identically zero. These systems are difficult to control due to limitations on plant inversion.

Systems with unstable zero dynamics are especially difficult to control when the zero dynamics are unknown. This case occurs in hypersonic vehicles, whose zero dynamics are poorly modeled due to the complex aerodynamics [2]–[6].

The present paper applies indirect adaptive control to systems with uncertain, unstable zero dynamics. The starting point for this work is retrospective cost adaptive control (RCAC), which is a discrete-time adaptive control technique that is applicable to stabilization, command following, and disturbance rejection. RCAC is described in [7], [8], and various applications are considered in [9]–[11].

The modeling information needed by RCAC is used to specify the target model $G_{\rm f}$, which defines the retrospective cost function. In the SISO case, the required minimal modeling information is the relative degree, the sign of the leading numerator coefficient, and any NMP zeros. In the MIMO case, the required minimal modeling information needed to specify $G_{\rm f}$ is an open problem.

In practice, however, a plant may be NMP, but the NMP zeros may be uncertain. If the plant has NMP zeros that are poorly modeled, then RCAC may or may not cancel them, depending on the accuracy of the knowledge of the NMP zeros as well as the aggressiveness of the controller. The tendency of RCAC to cancel NMP zeros is exploited in [12], where unstable pole locations are used as estimates of the NMP zeros.

Syed Aseem Ul Islam, Tam W. Nguyen, Ilya V. Kolmanovsky, and Dennis S. Bernstein are with the Department of Aerospace Engineering, University of Michigan, Ann Arbor, MI, USA. {aseemisl, twnguyen, ilya, dsbaero}@umich.edu

The present paper extends RCAC to address the problem of unknown NMP zeros, especially for the MIMO case. This approach, called data-driven retrospective cost adaptive control (DDRCAC) [13], uses online system identification to construct $G_{\rm f}$. In particular, closed-loop identification using recursive least squares (RLS) is used to identify an infinite-impulse-response (IIR) model whose numerator is used to update a finite-impulse-response (FIR) target model $G_{{\rm f},k}$ at each step. This technique can be applied to both SISO and MIMO systems. This paper develops DDRCAC and applies this technique to linear NMP systems as well as nonlinear systems with unstable nonlinear zero dynamics.

Since DDRCAC relies on online identification, we investigate the effect of the sensor noise on the closed-loop performance. In order to examine this sensitivity, we apply DDRCAC to a system with an unknown NMP zero with increasing levels of sensor noise. Furthermore, we present an example in which the transients that arise due to poor identification lead to improved identification accuracy, which, in turn, facilities closed-loop control using DDRCAC.

II. Command-Following Problem

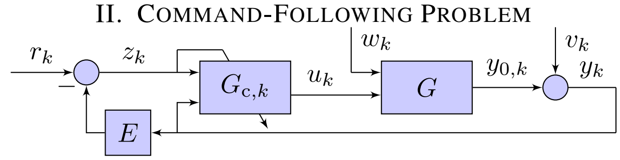

Fig. 1: Block diagram representation of the adaptive servo problem. The objective is to have the performance variable Ey_k follow commands r_k, where E is a matrix that selects the components of the measurement y_k. The adaptive controller $G_{{\rm c},k}$ has access to noisy measurements $y_k = y_{0,k} + v_k$ and the adaptation variable $z_k = r_k - Ey_k$, and computes u_k. The plant G is acted upon by u_k and w_k, and produces the output $y_{0,k}$.

We consider the servo loop shown in Figure 1, where r_k is the command and w_k is the disturbance. The plant output is $y_{0,k}$, and the measurement is given by $y_k = y_{0,k} + v_k$, where v_k is sensor noise. The performance variable is the signal Ey_k, where the matrix E selects components of y_k that are required to follow the command r_k. The command-following error is thus $z_k \stackrel{\triangle}{=} r_k - Ey_k$. The inputs to the adaptive feedback controller $G_{{\rm c},k}$ are the measurement y_k and the command-following error z_k. Note that z_k also serves as the adaptation variable, as denoted by the diagonal line passing through $G_{{\rm c},k}$. The objective is to minimize the adaptation variable, that is, the command-following error, in the presence of the disturbance and sensor noise.

Note that the servo loop in Figure 1 involves two plants in feedback, namely, G and EG. In practice, each of these plants may be either minimum phase or nonminimum phase, and the presence of NMP zeros in either plant may impact robustness and achievable performance. In the special case where y_k is the full state of G, it follows that G has no zeros and thus is minimum phase. In the present paper, we focus exclusively on the output-feedback case where G is NMP and $EG = G$. Furthermore, $r_k \in \mathbb{R}^p, y_k \in \mathbb{R}^p, z_k \in \mathbb{R}^p$, and $u_k \in \mathbb{R}^m$.

The plant G is modeled as the strictly-proper discrete-time input-output (IO) system

$$y_{0,k} = -\sum_{i=1}^{n} A_i y_{0,k-i} + \sum_{i=\ell}^{n} B_i u_{k-i} + w_{k-1}, \qquad (1)$$

$$y_k = y_{0,k} + v_k, \qquad (2)$$

where k is the step, n is the system window length, $y_{0,k} \in \mathbb{R}^p$ is the output, $y_k \in \mathbb{R}^p$ is a noisy measurement of $y_{0,k}$, $u_k \in \mathbb{R}^m$ is the control, $w_k \in \mathbb{R}^p$ is the disturbance, $0 < \ell < n$ is an integer, and $A_i \in \mathbb{R}^{p\times p}$, $B_i \in \mathbb{R}^{p\times m}$ are system coefficient matrices. In the cases $w_k = 0$, $v_k = 0$,

$$G(\mathbf{q}) \triangleq \Big(I_p \mathbf{q}^n + \sum_{i=1}^{n} A_i \mathbf{q}^{n-i}\Big)^{-1} \sum_{i=\ell}^{n} B_i \mathbf{q}^{n-i}, \qquad (3)$$

is the transfer-function from u_k to y_k, where $\mathbf{q}$ is the forward-shift operator.

III. Data-Driven Retrospective Cost Adaptive Control

DDRCAC consists of two components, namely, online identification and RCAC. The online identification uses RLS to fit an IIR IO model using y_k and u_k data obtained during closed-loop operation. A second implementation of RLS is used to update the RCAC adaptive controller using a target model constructed from the latest identified model. In particular, at each step we construct the target model $G_{\mathrm{f},k}$ as an FIR filter whose numerator is identical to the numerator of the latest identified IIR model. Both RLS implementations use data-dependent variable-rate forgetting (VRF). The following result is RLS with VRF from [14] that is used to implement DDRCAC.

Proposition 1: For all $k \geq 0$, let $Y_k \in \mathbb{R}^{l_Y}$, $\Phi_k \in \mathbb{R}^{l_Y \times l_\Theta}$, $\lambda_k \in (0,1]$, and define $\rho_k \triangleq \prod_{j=0}^{k} \lambda_j$. Let $\Theta_0 \in \mathbb{R}^{l_\Theta}$, and let $P_0 \in \mathbb{R}^{l_\Theta \times l_\Theta}$ be positive definite. Furthermore, for all $k \geq 0$, denote the minimizer of

$$J_k(\Theta) \triangleq \sum_{i=0}^{k} \frac{\rho_k}{\rho_i}(Y_i - \Phi_i\Theta)^{\mathrm{T}}(Y_i - \Phi_i\Theta) + \rho_k(\Theta - \Theta_0)^{\mathrm{T}} P_0^{-1}(\Theta - \Theta_0). \qquad (4)$$

where $\Theta \in \mathbb{R}^{l_\Theta}$, by $\Theta_{k+1} \triangleq \underset{\Theta \in \mathbb{R}^{l_\Theta}}{\operatorname{argmin}} J_k(\Theta)$. Then, for all $k \geq 0$, Θ_{k+1} is given by

$$P_{k+1} = \tfrac{1}{\lambda_k} P_k - \tfrac{1}{\lambda_k} \Phi_k^{\mathrm{T}}(\lambda_k I_{l_Y} + \Phi_k P_k \Phi_k^{\mathrm{T}})^{-1}\Phi_k P_k, \qquad (5)$$

$$\Theta_{k+1} = \Theta_k + P_{k+1}\Phi_k^{\mathrm{T}}(Y_k - \Phi_k\Theta_k). \qquad (6)$$

A. Online Identification

We fit a strictly-proper linear IO model of the form

$$y_k = -\sum_{i=1}^{\eta} F_{i,k} y_{k-i} + \sum_{i=1}^{\eta} G_{i,k} u_{k-i}, \qquad (7)$$

to y_k and u_k, where η is the model window length, and $F_i \in \mathbb{R}^{p\times p}$ and $G_i \in \mathbb{R}^{p\times m}$ are the model coefficient matrices that are to be updated. To perform this update recursively we define the plant identification error

$$z_{\mathrm{p},k}(\theta_{\mathrm{p}}) \triangleq y_k - \phi_{\mathrm{p},k}\theta_{\mathrm{p}}, \ \ \phi_{\mathrm{p},k} \triangleq \begin{bmatrix} -y_{k-1} \\ \vdots \\ -y_{k-\eta} \\ u_{k-1} \\ \vdots \\ u_{k-\eta} \end{bmatrix}^{\mathrm{T}} \otimes I_p \in \mathbb{R}^{p\times l_{\theta_{\mathrm{p}}}}, \qquad (8)$$

$$\theta_{\mathrm{p},k} \triangleq \mathrm{vec}\,[\, F_{1,k} \ \cdots \ F_{\eta,k} \ G_{1,k} \ \cdots \ G_{\eta,k} \,] \in \mathbb{R}^{l_{\theta_{\mathrm{p}}}}, \qquad (9)$$

The cost (4) with $Y_k - \Phi_k\Theta = z_{\mathrm{p},k}(\theta_{\mathrm{p}})$ is minimized using Proposition 1 with

$$Y_k \triangleq y_k, \quad \Phi_k \triangleq \phi_{\mathrm{p},k}, \quad \Theta \triangleq \theta_{\mathrm{p}}, \quad \lambda_k \triangleq \lambda_{\mathrm{p},k}, \qquad (10)$$

which recursively produces the minimizer $\theta_{\mathrm{p},k+1}$.

B. Retrospective Cost Adaptive Control

Define the dynamic compensator

$$u_k \triangleq \mathrm{sat}_\alpha(\phi_k\theta_{\mathrm{c},k}), \ \ \phi_k \triangleq \begin{bmatrix} u_{k-1} \\ \vdots \\ u_{k-n_{\mathrm{c}}} \\ y_{k-1} \\ \vdots \\ y_{k-n_{\mathrm{c}}} \end{bmatrix}^{\mathrm{T}} \otimes I_m \in \mathbb{R}^{m\times l_\theta}, \qquad (11)$$

n_{c} is the controller window length, $l_\theta = n_{\mathrm{c}} m(m+p)$, and $\theta_{\mathrm{c},k}$ is a vector of controller coefficients to be optimized. The definition (11) represents an IIR controller whose output is saturated by a multivariable saturation function sat_α. In particular, each entry x_i of a vector x is independently saturated by the corresponding entry α_i of α, to produce each entry $\mathrm{sat}_{\alpha_i}(x_i)$ of $\mathrm{sat}_\alpha(x)$. That is

$$\mathrm{sat}_{\alpha_i}(x_i) \triangleq \begin{cases} x_i, & |x_i| < \alpha_i, \\ \mathrm{sign}(x_i)\alpha_i, & |x_i| \geq \alpha_i. \end{cases} \qquad (12)$$

Next, define the retrospective cost variable

$$\hat{z}_k(\theta_{\mathrm{c}}) \triangleq z_k + N_k\bar{\phi}_k\theta_{\mathrm{c}} - N_k\bar{U}_k \in \mathbb{R}^p, \qquad (13)$$

which, assuming that R_u and $R_{\Delta u}$ are nonzero, is stacked with

$$-R_u\phi_k\theta_{\mathrm{c}} \in \mathbb{R}^m, \quad R_{\Delta u}(u_{k-1} - \phi_k\theta_{\mathrm{c}}) \in \mathbb{R}^m, \qquad (14)$$

where

$$\bar{\phi}_k \triangleq \begin{bmatrix} \phi_{k-1} \\ \vdots \\ \phi_{k-\eta} \end{bmatrix} \in \mathbb{R}^{\eta m\times l_\theta}, \quad \bar{U}_k \triangleq \begin{bmatrix} u_{k-1} \\ \vdots \\ u_{k-\eta} \end{bmatrix} \in \mathbb{R}^{\eta m}, \qquad (15)$$

$$N_k \triangleq \begin{cases} [\, -1_{p\times m} \ 0 \ \cdots \ 0 \,], & G_{i,k+1} = 0, \\ [\, -G_{1,k+1} \ \cdots \ -G_{\eta,k+1} \,], & \text{otherwise}, \end{cases} \qquad (16)$$

$$z_k \triangleq r_k - y_k, \qquad (17)$$

$R_u \in \mathbb{R}^{m\times m}$ is the positive-semidefinite control weighting, $R_{\Delta u} \in \mathbb{R}^{m\times m}$ is the positive-semidefinite control move weighting, $G_{i,k+1} \in \mathbb{R}^{p\times m}$ for $i = 1,\ldots,\eta$ are the numerator coefficients of the identified model, $N_k \in \mathbb{R}^{p\times \eta m}$, $r_k \in \mathbb{R}^p$ is the command, and $z_k \in \mathbb{R}^p$ is the command-following error and the adaptation variable. Note that the identification update at step k can be performed before the adaptive control update and thus $G_{i,k+1}$ are available for the construction of N_k at step k. The cost (4) with $Y_k - \Phi_k\Theta = \hat{z}_k(\theta_{\rm c})$ is minimized using Proposition 1 with

$$Y_k \triangleq z_k - N_k\bar{U}_k \in \mathbb{R}^p, \tag{18}$$

which, assuming that R_u and $R_{\Delta u}$ are nonzero, is stacked with

$$0 \in \mathbb{R}^m, \quad R_{\Delta u}u_{k-1} \in \mathbb{R}^m, \tag{19}$$

and

$$\Phi_k \triangleq -N_k\bar{\phi}_k \in \mathbb{R}^{p\times l_\theta}, \tag{20}$$

which, assuming that R_u and $R_{\Delta u}$ are nonzero, is stacked with

$$R_u\phi_k \in \mathbb{R}^{m\times l_\theta}, \quad R_{\Delta u}\phi_k \in \mathbb{R}^{m\times l_\theta}, \tag{21}$$

and $\Theta \triangleq \theta_{\rm c}$, $\lambda_k \triangleq \lambda_{{\rm c},k}$, which recursively produces the minimizer $\theta_{{\rm c},k+1}$.

For all examples in this paper, $\theta_{{\rm p},k}$ and $\theta_{{\rm c},k}$ are initialized as 0 in order to reflect the absence of additional prior modeling information. In addition, for both implementations of RLS $P_0 = p_0 I_{l_\Theta}$ where $p_0 > 0$ is a tuning hyperparameter.

C. Data-Dependent Variable Rate Forgetting

For data-dependent variable-rate forgetting, we define

$$\lambda_{{\rm p},k} \triangleq \frac{1}{1+\gamma f_{\tau_1,\tau_2,k}[z_{{\rm p},k}(\theta_{{\rm p},k})]}, \ \lambda_{{\rm c},k} \triangleq \frac{1}{1+\gamma f_{\tau_1,\tau_2,k}(z_k)}, \tag{22}$$

which are the time-varying data-dependent plant-identification and control forgetting factors, respectively, where

$$f_{\tau_1,\tau_2,k}(x_k) \triangleq \begin{cases} \frac{\xi_{\rm n}}{\xi_{\rm d}} - 1, & \frac{\xi_{\rm n}}{\xi_{\rm d}} > 1, \\ 0, & \frac{\xi_{\rm n}}{\xi_{\rm d}} \le 1 \text{ or } \xi_{\rm d} = 0, \end{cases} \tag{23}$$

$$\xi_{\rm n} \triangleq \left(\frac{1}{\tau_1}\sum_{i=k-\tau_1}^{k} x_i^{\rm T}x_i\right)^{1/2}, \xi_{\rm d} \triangleq \left(\frac{1}{\tau_2}\sum_{i=k-\tau_2}^{k} x_i^{\rm T}x_i\right)^{1/2}, \tag{24}$$

x_k is a vector and $\tau_1 < \tau_2$ are integers. The terms $\xi_{\rm n}$ and $\xi_{\rm d}$ are the average norms of x_k over periods of length τ_1 and τ_2, respectively. The integer τ_2 is chosen to be large so that $\xi_{\rm d}$ approximates the long-term variation of the x_k, whereas τ_1 is chosen to be small so that $\xi_{\rm n}$ approximates the short-term variation of the x_k, Consequently, the case $\frac{\xi_{\rm n}}{\xi_{\rm d}} > 1$ implies that the variation of x_k is greater in the recent past than over a longer time interval. The function f is used in DDRCAC to suspend forgetting when the variation of the error drops below a threshhold determined by the ratio $\frac{\xi_{\rm n}}{\xi_{\rm d}}$. This technique thus prevents DDRCAC from forgetting due to sensor noise rather than due the magnitude of the noise-free command-following error. A list of hyperparameters to be selected for DDRCAC is presented in Table I.

Parameter	Description	Selection
η	Model window length	Integer ≥ 1
$n_{\rm c}$	Controller window length	Integer ≥ 1
R_u	Control weighting	r_uI_m, $r_u \geq 0$
$R_{\Delta u}$	Control move weighting	$r_{\Delta u}I_m$, $r_{\Delta u} \geq 0$
α	Control saturation level vector	Actuator saturation
p_0	Initial RLS covariance scaling	$p_0 > 0$
γ	Forgetting parameter	$0 \leq \gamma < 1$
τ_1, τ_2	Forgetting window lengths	Integers $\tau_2 > \tau_1$

TABLE I: Tuning hyperparameters that need to be selected for DDRCAC.

IV. Application to NMP Systems

In this section, DDRCAC is applied to NMP systems. The first example is SISO and unstable, and the second example is MIMO and asymptotically stable. Within the context of the linear discrete-time IO model (1), NMP zeros are associated with the zero dynamics. In particular, if the first nonzero coefficient B_ℓ in (1) has full column rank, then setting $y_{0,k} \equiv 0$ and $w_k \equiv 0$ in (1) yields the zero dynamics

$$u_k = -(B_\ell^{\rm T}B_\ell)^{-1}B_\ell^{\rm T}\sum_{i=\ell+1}^{n} B_iu_{k+\ell-i}. \tag{25}$$

G has a NMP transmission zero if and only if the zero dynamics (25) are unstable.

Example 1. *Harmonic command following for an unstable SISO NMP system with step-disturbance rejection.* Consider the discrete-time, IO system

$$y_{0,k} = 1.4y_{0,k-1} - 1.1y_{0,k-2} + u_{k-1} - 1.3u_{k-2} + w_{k-1}, \tag{26}$$

which has the unstable linear zero dynamics

$$u_k = 1.3u_{k-1}. \tag{27}$$

Hence (26) has unstable poles $0.7 \pm 0.781\jmath$ rad/sample and NMP zero 1.3 rad/sample. The disturbance w_k is a step of height 0.5, the sensor noise v_k is a zero-mean Gaussian sequence with standard deviation 0.001, and the command is $r_k = \sin 0.23k$. For DDRCAC we set $\eta = 2$, $n_{\rm c} = 8$, $R_u = R_{\Delta u} = 0$, $\alpha = 3$, $p_0 = 10^4$, $\gamma = 0.1$, $\tau_1 = 30$, and $\tau_2 = 100$. Figures 2, 3 show that the harmonic command is followed asymptotically and the disturbance is rejected.

To investigate the inter-dependence between online-identification and RCAC we repeat the example with $p_0 = 10^{-4}$. This value of p_0 corresponds to less aggressive identification and control. Consequently, poor identification of the true plant is expected, which in turn is expected to result in poor closed-loop performance. Figure 4(a) shows a large transient in y_k between $k = 43$ and $k = 110$ that corresponds to poor command-following performance. The poor command-following performance is a result of the insufficient modeling information in $G_{{\rm f},43}$, which in turn is due to the poor model of the system at $k = 43$, as shown in Figure 4(d). The transient in y_k causes a large change in the identification coefficients between $k = 43$ and $k = 80$, as shown in Figure 4(b), which leads to an identified model at $k = 71$ that approximately captures the poles of the true system, as shown in Figure 4(e). The large change in the identification coefficients causes a large change in the controller coefficients between $k = 71$ and $k = 110$ as shown in Figure 4(c). At $k = 110$ the identified model captures the poles and NMP zero of the true system as shown in Figure 4(f) and thus, for $k > 110$ $G_{\mathrm{f},k}$ contains the modeling information required by RCAC. Consequently, for $k > 110$ asymptotic command following is achieved. The poles and zeros of the plant and identified model are shown in Figure 4(d)–(f) at $k = 43$, $k = 71$, and $k = 110$. This investigation shows that, when the model is poor, the resulting transient response of y_k provides additional persistence of excitation, which enhances identification accuracy.

Next, we repeat the example with varying levels of sensor noise. The absolute error from these simulations, and the poles and zeros of the identified model are shown in Figure 5. Increasing levels of sensor noise degrade the identification of the poles and zeros, and thus the performance of DDRCAC. Note that, although the accuracy of the identified poles and zeros is poor in the case $\sigma(v_k) = 1$, closed-loop stability is maintained. ◇

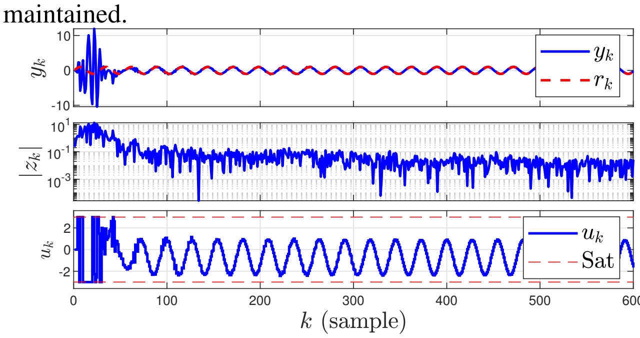

Fig. 2: Example 1: Harmonic-command following and step-disturbance rejection for an unstable SISO NMP system. The signal-to-noise ratio between y_k and v_k is 64 dB.

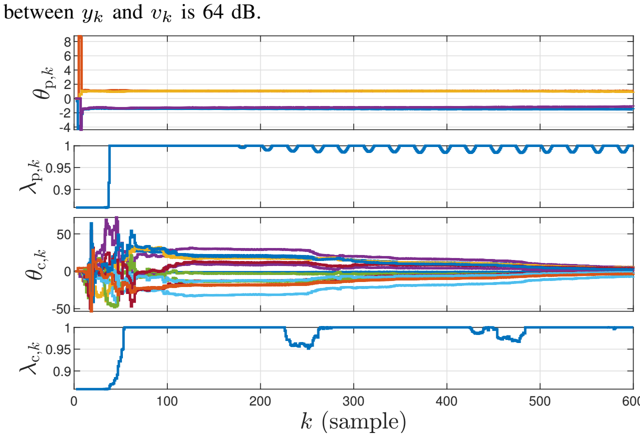

Fig. 3: Example 1: Harmonic-command following and step-disturbance rejection for an unstable SISO NMP system. The identification coefficients, identification forgetting factor, controller coefficients, and controller forgetting factor are shown.

Example 2. *Multi-step command following for an asymptotically stable MIMO NMP system.* Consider (1) with

$$A_1 = I_2, A_2 = \begin{bmatrix} 0.3 & 0 \\ 0 & 0.4 \end{bmatrix}, B_1 = \begin{bmatrix} -1 & 4 \\ 3 & 6 \end{bmatrix}, B_2 = \begin{bmatrix} 3.2 & -0.8 \\ -0.6 & -1.2 \end{bmatrix}. \tag{28}$$

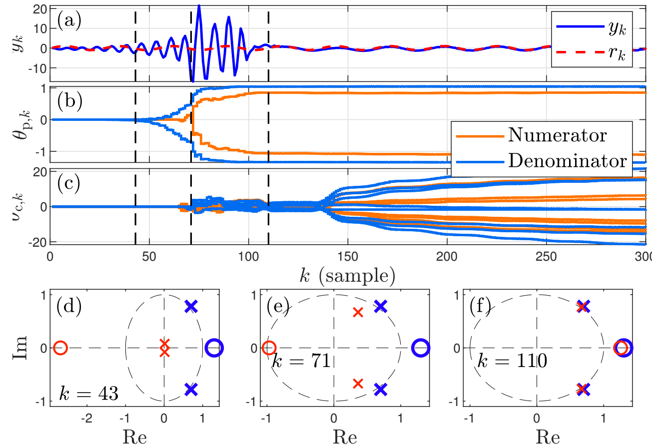

Fig. 4: Example 1: Harmonic-command following and step-disturbance rejection for an unstable SISO NMP system using a small value p_0. (a) shows that, between $k = 43$ and $k = 110$, the command-following error has a large transient. (b) shows that, due to the transient in y_k, the identification coefficients undergo a large change between $k = 43$ and $k = 80$. Note that, the update of the numerator of the identified model lags the update of the identification of the denominator. (c) shows that, due to the large change in the identification coefficients, the controller coefficients undergo a large change between $k = 71$ and $k = 110$. (d), (e), and (f) show the poles and zeros of the true system (blue) and the identified model (red) at $k = 43$, $k = 71$, and $k = 110$, respectively.

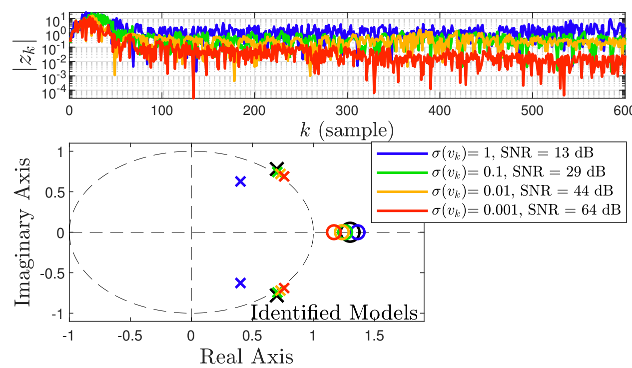

Fig. 5: Example 1: Harmonic-command following and step-disturbance rejection for an unstable SISO NMP system. The absolute command-following error $|z_k|$ is shown for four cases with different levels of sensor noise $\sigma(v_k)$. Higher levels of sensor noise degrade closed-loop performance. The poles and zeros of the identified model at the end of each simulation are also shown. The poles and zeros of the true system are shown in black.

The transmission zeros, channel zeros, and poles of G are shown in Figure 6. G has NMP channel and transmission zeros, and is asymptotically stable. Using (25) the zero dynamics for this system are given by $u_k = \begin{bmatrix} 1.2 & 0 \\ -0.5 & 0.2 \end{bmatrix} u_{k-1}$. Note that the eigenvalues of the matrix that defines the zero dynamics are 0.2 and 1.2 which are the transmission zeros of G. The disturbance w_k and sensor noise v_k are zero-mean Gaussian sequences with standard deviation 0.001 and 0.01, respectively, and the command is given by

$$r_k = \begin{cases} r_1, & 0 \le k < 150, \\ r_2, & 150 \le k < 300, \\ r_3, & 300 \le k < 450, \\ r_4, & k \ge 450, \end{cases} \tag{29}$$

$$r_1 \triangleq \begin{bmatrix} 0.2 \\ 0 \end{bmatrix}, \ r_2 \triangleq \begin{bmatrix} 1.5 \\ 1.25 \end{bmatrix}, \ r_3 \triangleq \begin{bmatrix} -1.25 \\ -1.5 \end{bmatrix}, \ r_4 \triangleq \begin{bmatrix} -0.25 \\ 0.15 \end{bmatrix}. \tag{30}$$

For DDRCAC we set $\eta = 2$, $n_\mathrm{c} = 8$, $R_u = R_{\Delta u} = 0$, $\alpha = [\ 0.25\ 0.25\ ]^\mathrm{T}$, $p_0 = 10^4$, $\gamma = 0.1$, $\tau_1 = 30$, and $\tau_2 = 100$. Figures 7, 8 show that the multi-step command is followed asymptotically. ◇

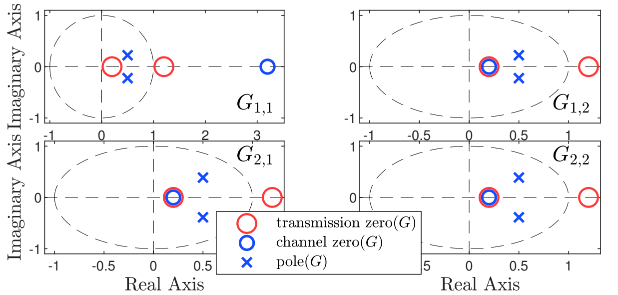

Fig. 6: Example 2: Transmission zeros, channel zeros, and poles of the system where $G_{i,j}$ is the (i, j) entry of the MIMO transfer function G.

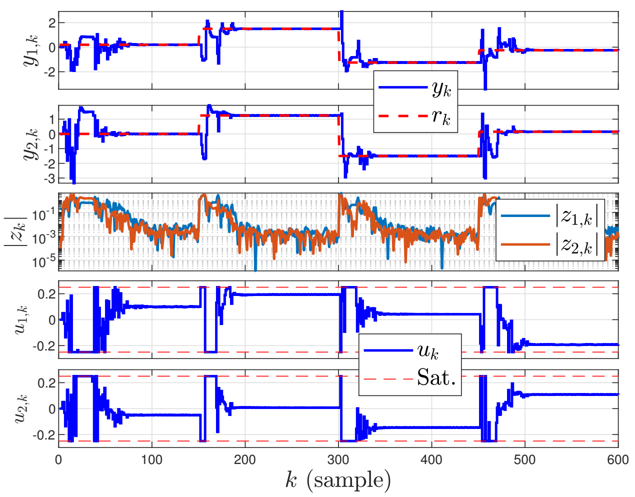

Fig. 7: Example 2: Multi-step command following for an asymptotically stable MIMO NMP system. The signal-to-noise ratio between y_k and v_k is $[\ 40\ 41\ ]^\mathrm{T}$ dB. The control u_k and the control saturation levels are shown.

V. Application to Nonlinear IO Systems with Nonlinear Unstable Zero Dynamics

In this section, DDRCAC is applied to nonlinear discrete-time IO systems of the form

$$y_{0,k} = -\sum_{i=1}^{n} A_i y_{0,k-i} + B_\ell u_{k-\ell} + h(u_{k-1-\ell}, \ldots, u_{k-n}) + w_{k-1}, \tag{31}$$

$$y_{k+1} = y_{0,k+1} + v_{k+1}, \tag{32}$$

where $0 < \ell < n$ is an integer, and $h\colon \mathbb{R}^m \times \cdots \times \mathbb{R}^m \to \mathbb{R}^p$. The first example is SISO and asymptotically stable, and the second example is MIMO and unstable. Both examples have nonlinear unstable zero dynamics. If B_ℓ has full column rank, then setting $y_{0,k} \equiv 0$ and $w_k \equiv 0$ yields the zero dynamics

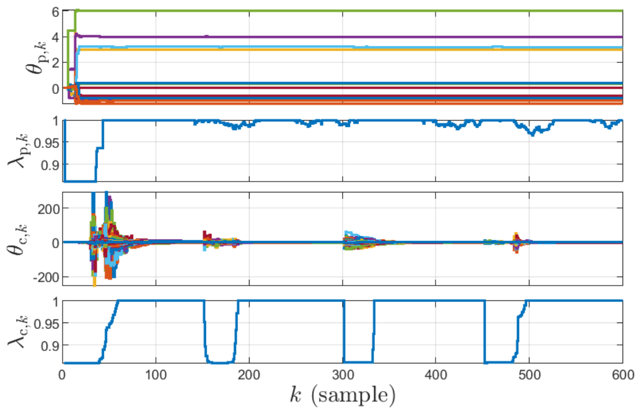

Fig. 8: Example 2: Multi-step command following for an asymptotically stable MIMO NMP system. The identification coefficients, identification forgetting factor, controller coefficients, and controller forgetting factor are shown.

$$u_k = -(B_\ell^\mathrm{T} B_\ell)^{-1} B_\ell^\mathrm{T} h(u_{k-1}, \ldots, u_{k+\ell-n}). \tag{33}$$

Note that, despite the fact that the examples in this section have nonlinear zero dynamics, the identification model (7) is linear.

Example 3. *Multi-step command following for an asymptotically stable SISO system with unstable nonlinear zero dynamics.* Consider the discrete-time, IO system

$$y_{0,k} = 0.9 y_{0,k-1} - u_{k-2} + u_{k-3} + u_{k-3}^3 + w_{k-1}. \tag{34}$$

This system has unstable nonlinear zero dynamics

$$u_k = (1 + u_{k-1}^2) u_{k-1}, \tag{35}$$

and is open loop unstable. The disturbance w_k and sensor noise v_k are zero-mean Gaussian sequences with standard deviation 0.001 and 0.01, respectively, and the command is

$$r_k = \begin{cases} 1, & 0 \le k < 300, \\ -1, & k \ge 300. \end{cases} \tag{36}$$

For DDRCAC we set $\eta = 3$, $n_\mathrm{c} = 8$, $R_u = 0$, $R_{\Delta u} = 0.3$, $\alpha = 1$, $p_0 = 10^4$, $\gamma = 0.1$, $\tau_1 = 30$, and $\tau_2 = 100$. Figures 9, 10 show that the multi-step command is followed asymptotically. ◇

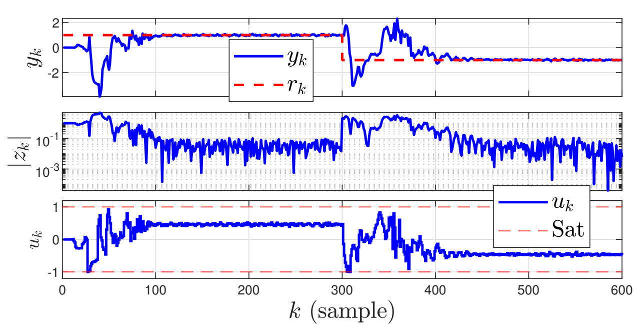

Fig. 9: Example 3: Multi-step command following for an asymptotically stable SISO system with unstable nonlinear zero dynamics. The signal-to-noise ratio between y_k and v_k is 40 dB.

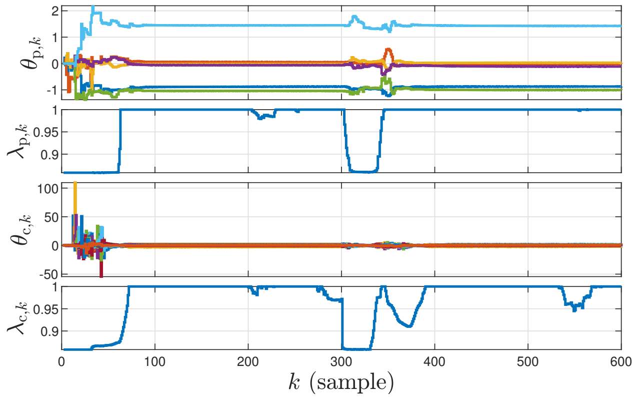

Fig. 10: Example 3: Multi-step command following for an asymptotically stable SISO system with unstable nonlinear zero dynamics. The identification coefficients, identification forgetting factor, controller coefficients, and controller forgetting factor are shown.

Example 4. *Multi-step command following for an unstable MIMO system with unstable nonlinear zero dynamics and harmonic disturbance rejection.* Consider (31) with

$$A_1 = \begin{bmatrix} -0.4 & -1 \\ 0 & -1.1 \end{bmatrix}, \quad B_1 = \begin{bmatrix} 1 & 0 \\ 0 & 1 \end{bmatrix}, \tag{37}$$

$$h(u_{k-1}) = \begin{bmatrix} |\sin u_{1,k-1}|u_{1,k-1} + u_{2,k-1} \\ |\cos u_{2,k-1}|u_{2,k-1} \end{bmatrix}. \tag{38}$$

Note that the system is open-loop unstable. Using (25) the unstable nonlinear zero dynamics for this system are given by $u_k = \begin{bmatrix} |\sin u_{1,k-1}| & 1 \\ 0 & |\cos u_{2,k-1}| \end{bmatrix} u_{k-1}$. The harmonic disturbance is given by $w_k = 0.05 \sin 0.33k$, the sensor noise v_k is a zero-mean Gaussian sequence with standard deviation 0.01, and the command is given by (30). For DDRCAC we set $\eta = 2$, $n_\mathrm{c} = 8$, $R_u = R_{\Delta u} = 0$, $\alpha = [\ 0.6\ 0.6\ ]^\mathrm{T}$, $p_0 = 10^4$, $\gamma = 0.2$, $\tau_1 = 30$, and $\tau_2 = 100$. Figures 11–12 show that the multi-step command is followed asymptotically and the harmonic disturbance is rejected. $\diamond$

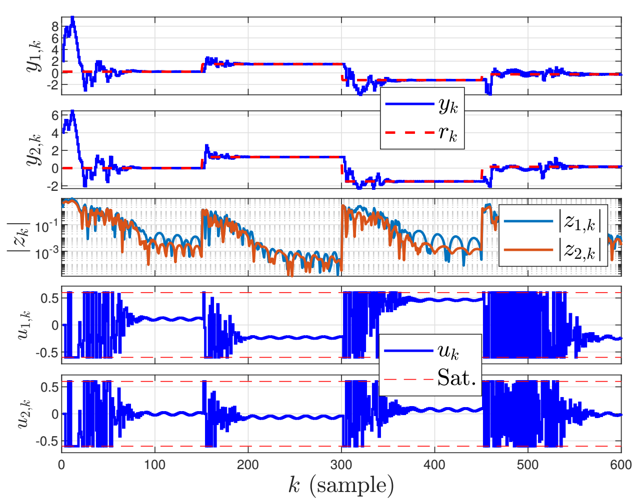

Fig. 11: Example 4: Multi-step command following and harmonic disturbance rejection for an unstable MIMO system with unstable nonlinear zero dynamics. The signal-to-noise ratio between y_k and v_k is $[\ 44\ 42\ ]^\mathrm{T}$ dB. The control u_k and the control saturation levels are shown.

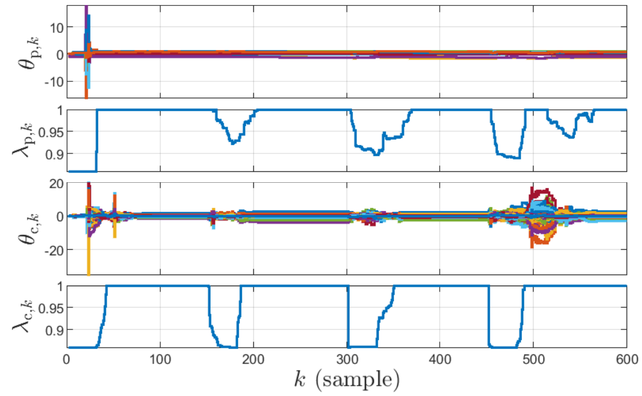

Fig. 12: Example 4: Multi-step command following and harmonic disturbance rejection for an unstable MIMO system with unstable nonlinear zero dynamics. The identification coefficients, identification forgetting factor, controller coefficients, and controller forgetting factor are shown.

VI. Acknowledgments

This research was supported by the Office of Naval Research under grant N00014-18-1-2211 of the BRC Program.

References

[1] S. A. Al-Hiddabi and N. H. McClamroch, "Tracking and maneuver regulation control for nonlinear nonminimum phase systems: application to flight control," *IEEE Trans. Contr. Sys. Tech.*, vol. 10, no. 6, pp. 780–792, Nov 2002.

[2] L. Fiorentini and A. Serrani, "Adaptive restricted trajectory tracking for a non-minimum phase hypersonic vehicle model," *Automatica*, vol. 48, no. 7, pp. 1248–1261, 2012.

[3] H. Xu, M. D. Mirmirani, and P. A. Ioannou, "Adaptive sliding mode control design for a hypersonic flight vehicle," *AIAA J. Guid. Contr. Dyn.*, vol. 27, p. 829–838, 2004.

[4] J. T. Parker, A. Serrani, S. Yurkovich, M. A. Bolender, and D. B. Doman, "Control-Oriented Modeling of an Air-Breathing Hypersonic Vehicle," *AIAA J. Guid. Contr. Dyn.*, vol. 30, no. 3, pp. 856–869, 2007.

[5] H. Buschek and A. J. Calise, "Uncertainty Modeling and Fixed-Order Controller Design for a Hypersonic Vehicle Model," *AIAA J. Guid. Contr. Dyn.*, vol. 20, no. 1, pp. 42–48, 1997.

[6] M. A. Bolender and D. B. Doman, "Nonlinear Longitudinal Dynamical Model of an Air-Breathing Hypersonic Vehicle," *AIAA J. Spacecraft Rockets*, vol. 44, no. 2, pp. 374–387, 2007.

[7] Y. Rahman, A. Xie, and D. S. Bernstein, "Retrospective Cost Adaptive Control: Pole Placement, Frequency Response, and Connections with LQG Control," *IEEE Contr. Sys. Mag.*, vol. 37, pp. 28–69, Oct. 2017.

[8] J. B. Hoagg and D. S. Bernstein, "Retrospective Cost Model Reference Adaptive Control for Nonminimum-Phase Systems," *J. Guid. Contr. Dyn.*, vol. 35, pp. 1767–1786, 2012.

[9] A. Ansari and D. S. Bernstein, "Retrospective Cost Adaptive Control of Generic Transport Model Under Uncertainty and Failure," *J. Aero. Info. Sys.*, vol. 14, no. 3, pp. 123–174, 2017.

[10] Z. Zhao, G. Cruz, and D. S. Bernstein, "Adaptive Spacecraft Attitude Control Using Single-Gimbal Control Moment Gyroscopes Without Singularity Avoidance," *J. Guid. Contr. Dyn.* available online, 2019.

[11] A. Xie and D. S. Bernstein, "Adaptive Feedback Noise Control for Wide, Square, and Tall Systems," in *Proc. Amer. Contr. Conf.*, July 2019, pp. 435–440.

[12] S. A. U. Islam, A. Xie, and D. S. Bernstein, "Adaptive Control of Systems with Unknown Nonminimum-Phase Zeros Using Cancellation-Based Pseudo-identification," in *Proc. Amer. Contr. Conf.*, July 2019, pp. 441–446.

[13] S. A. U. Islam, A. L. Bruce, T. W. Nguyen, I. Kolmanovsky, and D. Bernstein, "Adaptive Flight Control with Unknown Time-Varying Unstable Zero Dynamics," *AIAA Scitech*, 2020, AIAA 2020-0839.

[14] A. L. Bruce, A. Goel, and D. S. Bernstein, "Recursive Least Squares with Matrix Forgetting," in *Proc. Amer. Contr. Conf.*, July 2020.